JOURNAL OF MATERIALS SCIENCE 33 (1998) 155–159

Nanometre-sized silver halides entrapped in SiO_2 matrices

W. MATZ, M. T. PHAM, A. MÜCKLICH
Institute of Ion Beam Physics and Materials Research, Research Center Rossendorf Inc., PO Box 510119, D-01314 Dresden, Germany

The formation of nanocrystals after implantation of silver alone as well as together with the halogen ions Cl, Br and I into a SiO_2 layer of about 100 nm was studied by X-ray diffraction and transmission electron microscopy. The co-implantation of Ag and Cl or Br results in the formation of cubic AgX crystals which are stable in size under annealing. The co-implantation of Ag and I as well as single Ag implantation result in Ag crystallites, which grow under annealing. The annealing procedure causes a redistribution of the particles within the layer.

1. Introduction

Current research on clusters or nanocrystals is devoted to the understanding of changes in fundamental properties of particles consisting of some hundreds to many thousands of atoms. The electronic and optical properties are determined by the interplay of bulk bonding geometry of the atoms and the limited size. Surface states can be eliminated by enclosure in another material with a larger band gap (passivation) [1]. In the nanometre size range, metals and semiconductors exhibit surface-mediated plasmon resonance and quantum confinement effects [2]. Size-dependent changes in band-gap energy, excited-state electronic behaviour, and optical spectra are generated which differ drastically from those known for the molecular and bulk limits, respectively. The new characteristics make this class of materials attractive for a number of technological applications, including photonic devices, catalysis, corrosion protection, solar energy conversion, and chemical or biochemical sensors [3–6].

Preparation and characterization of nanocrystallites are critical for a fundamental understanding and tailoring of materials properties of practical use. Metallic silver and semiconducting silver halides are widely used as model materials for studying the size quantization effects and surface photochemistry of finely dispersed semiconducting particles. For silver colloids formed after implantion in SiO_2 a blue shift and increasing intensity of optical reflectance was reported [7]. Different investigations of AgBr and AgI have shown indirect exciton emission in the blue-light region of fluorescence spectra (see, for example, [8, 9]). The emission intensity is increased with reduction in crystallite size. It was suggested that the electronic properties of silver halides in general should be sensitive to crystallite size. Up to now, mostly colloidal solutions have been studied, and the liquid phase is impractical in many respects [6, 10–12]. The entrapment in solid hosts has been described for some matrices, e.g., glasses, polymers and zeolites [6, 10, 11, 13]. The problems encountered have been the limitations in concentration level and profile, the susceptibility to decomposition of compounds and the incompatibility with the standard planar technologies. Furthermore, the detailed mechanisms which govern the particle size, shape, concentration and stoichiometry are not yet fully understood.

We report the preparation of nanocrystallites of silver halides or silver by sequential ion implantation of silver and halogens into a host matrix of SiO_2. The great reactivity of halogens with silver, in competition with the high quenching rate of the implantation process and the insolubility of silver halides in SiO_2, results in some cases in the formation of silver halide particles embedded in the matrix host. The size and the nature of particles formed were investigated by X-ray diffraction (XRD) and transmission electron microscopy (TEM). Furthermore, the changes occurring after the samples had been annealed at different temperatures were studied.

2. Experimental procedure

Thin films (100 nm) of SiO_2 obtained by chemical vapour deposition (CVD) were used as host matrices. They were deposited on a single-crystal silicon substrate (orientation, (1 0 0), resistivity, 10–14 Ω cm) via a 100 nm barrier layer of Si_3N_4 and a 70 nm intermediate layer of SiO_2. Amorphous SiO_2 is chemically stable and does not crystallize by ion implantation. Silver and the halogen ions Cl, Br and I were implanted subsequently into the CVD SiO_2 layer with a unique dose of 6×10^{16} ions cm^{-2} corresponding to stochiometric AgX. During implantation the target temperature reached 170 °C by beam heating. The energies of Ag^+ (40 keV) and X^+ (25 keV Cl; 42 keV Br; 42 keV I) were determined from the TRIM code [14] in order to produce overlapping concentration

0022–2461 © 1998 Chapman & Hall

profiles in the CVD SiO_2 layer. Additionally, samples with a single implantation of silver were prepared. The projected range of the ions is about 30 nm in all cases. The subsequent thermal treatment was carried out in the temperature range from 400 to 900 °C for 10 min in a nitrogen atmosphere.

The XRD characterization of the samples was performed with an ordinary laboratory diffractometer using Cu Kα radiation (1.2 kW) and a thin-film attachment. The latter consists of a Soller collimator (0.4°) and a graphite monochromator in front of the detector. To achieve the required sensitivity to the surface layers the angle of incidence was kept constant at $\omega = 1°$. The penetration depth of X-rays in this configuration is high enough to investigate the whole multilayer. XRD spectra were collected with step size of 0.1° and a typical counting time of 25 s per point. The intrinsic peak width of the diffractometer with the thin-film attachment is 0.42°.

TEM was carried out using a 300 keV microscope with a bright-field image. For some representative samples the particles were inspected with high-resolution imaging. The cross-section samples were prepared in order to study the distribution particles across the multilayer on the Si substrate. Additionally, energy-dispersive X-ray analysis gave some information about the distribution of implanted species in the sample.

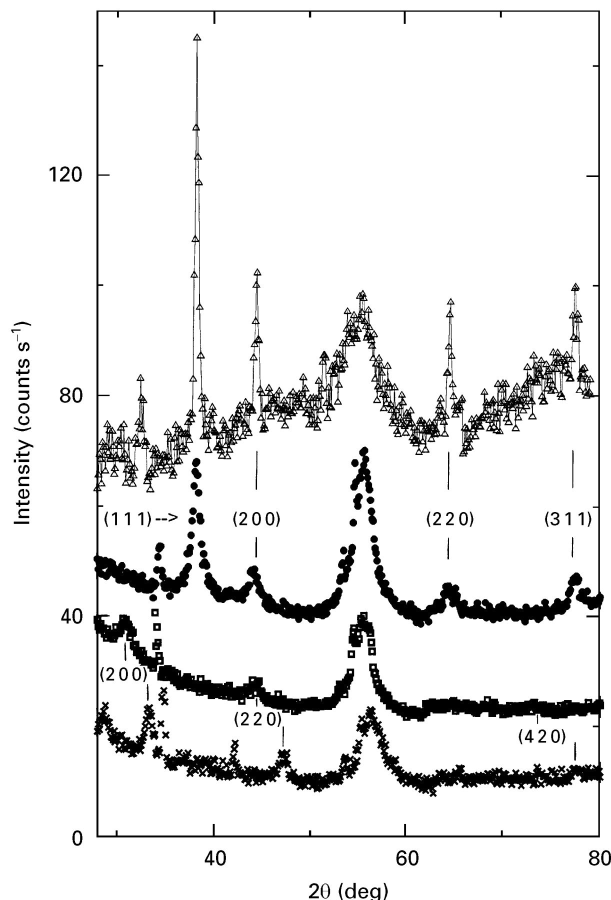

Figure 1 Representative XRD patterns from the implanted layers. In the case of single implantation of Ag (△) and co-implantation of Ag + 1 (●) their Bragg reflections of cubic Ag were observed. For the samples co-implanted with Ag + Br (□) and Ag + Cl (×), the Bragg reflections of the cubic NaCl type structure of AgBr and AgCl, respectively, occur. Unmarked peaks are substrate effects.

3. Results

3.1. X-ray diffraction

3.1.1. Phase formation

XRD survey patterns with 2θ between 25° and 80° were recorded for all samples. The phase identification results in the stochiometric compounds AgCl and AgBr for the samples co-implanted with silver and chlorine or bromine, respectively. After the co-implantation of silver and iodine the Bragg reflections of silver were observed. In the case of a single silver implantation, silver reflections could be identified. Fig. 1 shows representative diffraction patterns for the four implantation conditions. The Bragg reflections are indicated for the crystallites of the phases which were observed. Additional broad maxima around 57° and changing sharp peaks near 35° are assigned to scattering from the single-crystal silicon substrate.

While, in the case of co-implantation of Ag and halogens, typical Bragg reflections from crystals were observed already in the as-implanted samples, the single implanted silver sample has to be annealed up to 500 °C in order to exhibit Bragg reflections. In the as-implanted state there are no silver crystallites or they are too small to give Bragg peaks in XRD.

All detected phases are the normal condition cubic phases as tabulated in the "Powder diffraction file (PDF-2)" [15]. The relative deviation of the experimental lattice constants from the tabulated data is not greater than 0.002. AgBr and AgCl crystallize in the rock salt structure (NaCl or B1 type) and Ag in the face-centred cubic structure (A1). All Bragg reflections expected in the investigated 2θ region were observed.

3.1.2. Crystallite sizes from X-ray diffraction

The diffraction lines resulting from Ag, AgCl and AgBr are significantly broadened. This is an effect of crystallite size. Moreover, the broadening decreases dependent on the annealing temperature. The estimation of linewidth allows one to follow the growth of the particles.

The crystallite sizes were estimated for all samples from the line broadening of the first two or three sufficiently intense Bragg reflections (in the case of Ag, (1 1 1), (2 0 0) and (2 2 0); in the case of AgX, (2 0 0) and (2 2 0)). The reflections were fitted by Gaussians and the integral breadths of the peaks were corrected for instrumental linewidth. The crystallite size Λ itself was calculated from the Scherrer formula [16, 17] :

$$\Lambda = \frac{\lambda}{b^* \cos\theta}$$

Here, b is the line breadth corrected for instrumental resolution, λ the wavelength of X-rays and θ the Bragg angle.

A mean value of Λ was obtained from all reliable Bragg reflections. The estimated error takes into account the uncertainties in the fitting of the peaks with Gaussians as well as the averaging over all Bragg reflections.

The results for the mean crystallite size of all samples investigated are shown in Fig. 2. The as-implanted samples are indicated at 170 °C. This is the target temperature during implantation. For silver crystallites a dramatic temperature dependence of the size is observed. Contrary to that the AgCl and AgBr crystallites do not grow significantly at higher annealing temperatures.

3.2. Transmission electron microscopy

In the cross-section TEM the three-layer system on the Si crystal is always clearly visible. Nanosized particles were detected in the top layer of the system as demonstrated in Fig. 3. The particles appear as spheres with slightly different diameters. Furthermore one can estimate the thickness of the three layers from the micrographs. For the implantation of Ag, Ag + Br and Ag + Cl the layer thickness corresponds well to the nominal values. In contrast, after implantation of Ag + I the top SiO_2 layer has a thickness of only 67 nm, indicating significant sputtering during implantation. The effect of annealing the samples is visible in the particle size as well as in the particle distribution within the SiO_2 layer.

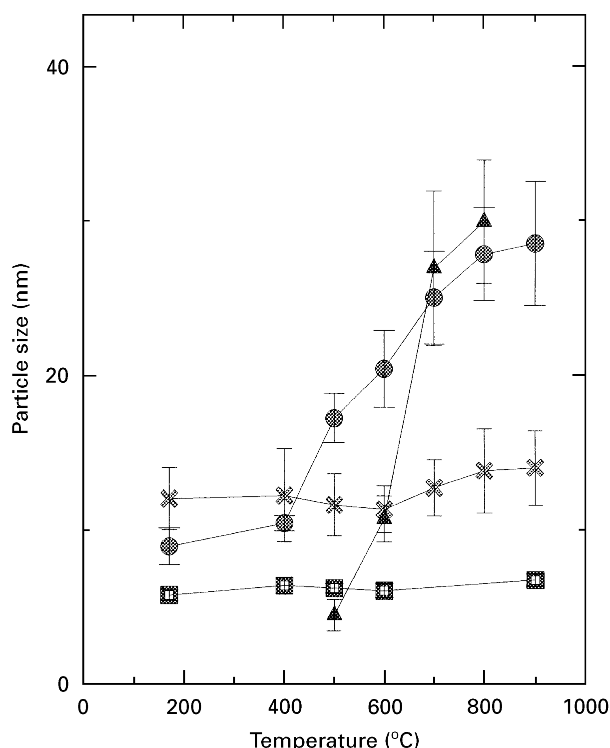

Figure 2 Mean size of cubic crystallites versus annealing temperature as deduced from the line broadening of the X-ray reflections. (▲), Ag (Ag crystals); (✕), Ag + Cl (AgCl crystals); (▣), Ag + Br (AgBr crystals); (●), Ag + I (Ag crystals). Depending on the specific implantation, pure Ag, AgBr and AgCl crystallites were observed.

For higher annealing temperatures, larger particles are observed. The size of the most frequent ("ordinary sized") particles corresponds well to the particle size deduced from XRD. Besides the ordinary sized particles, there exist very small particles (less than 3 nm) and a few huge particles. Here it should be mentioned that the coalescent growth of some particles under irradiation with an electron beam in the transmission electron microscope was observed for AgBr and AgCl. These growing particles become huge and seem to be located near the TEM sample surface. High-resolution TEM patterns of individual particles as shown in Fig. 4 for AgCl as a representative example give evidence that the ordinary sized particles are single crystallites whereas the huge particles are polycrystallites.

In the as-implanted samples, with the exception of the single Ag implantation, the particles are mostly located in the near-surface half of the SiO_2 layer. In the region near the Si_3N_4 layer, only some of the very small particles are observed (Fig. 3a). As a result of the anneal the particle distribution over the SiO_2 layer becomes more homogeneous (Fig. 3b) and tends to an enrichment of small particles near the SiO_2–Si_3N_4 interface at annealing temperatures above 800 °C (Fig. 3c). Obviously, the particles in all samples are entrapped in the SiO_2 layer. A temperature dependence of the evolution of the very small particles could not be observed, because they were masked by the redistribution of ordinary sized particles.

4. Discussion

For the estimation of the crystallite size the sample Scherrer formula was used. From the results of the TEM investigations we conclude that this procedure is justified, because spherical particles are observed which are mostly of a single-crystal nature. The particles are embedded in an amorphous matrix so that the strain effect as a source for the line-broadening

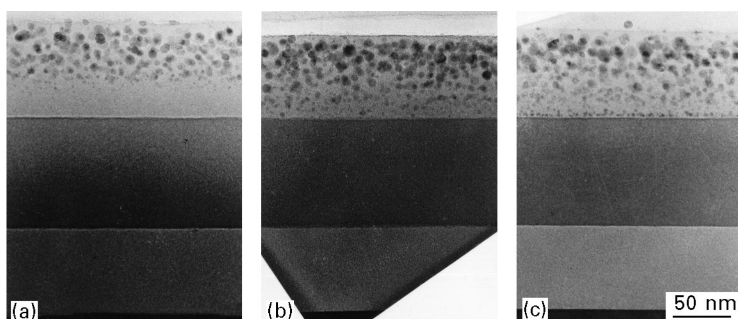

Figure 3 Cross-section TEM pictures of the AgBr particles after co-implantation of Ag and Br in the three-layer system (from the top, 100 nm of SiO_2, 100 nm of Si_3N_4 and 70 nm of SiO_2) on top of a silicon single-crystal substrate (black region at the bottom). The micrographs are taken for different annealing stages: (a) as implanted: (b) annealed at 600 °C, (c) annealed at 900 °C. The particles of AgBr are always located in the top layer of the SiO_2.

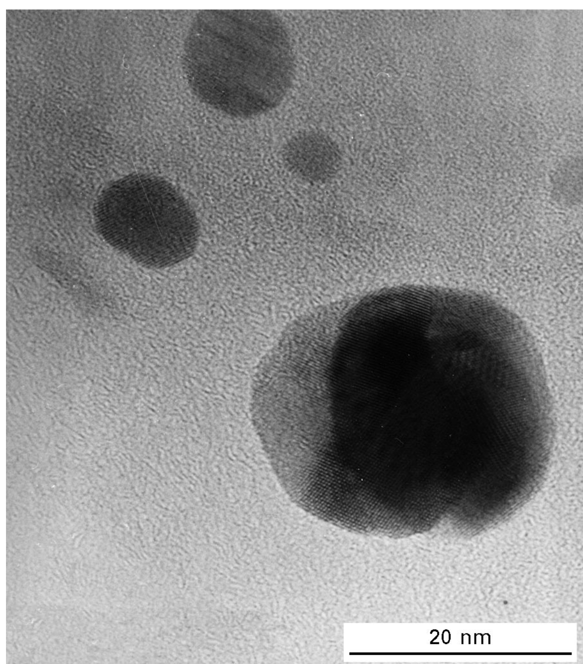

Figure 4 High-resolution TEM picture of ordinary sized particles (upper left region) and a huge particle (lower right region) observed in AgCl. The lattice planes within the crystallite demonstrate the single-crystallite and polycrystallite character of the smaller and the larger particles, respectively.

effects can be neglected. No strain contours were observed by TEM. Under the above-mentioned conditions, single Bragg line analysis is a good tool for particle size determination [17, 18]. Moreover, the direct size estimation from the TEM pattern confirms the X-ray results. The X-ray data are mean values from a sample surface area of about 15 mm × 6 mm. The X-ray method is unable to detect the very small particles below 3 nm size which have been observed by TEM. The great line broadening causes such a strong reduction in the peak height that no effect is observable with laboratory X-ray equipment. Since X-ray line broadening is sensitive to crystallite size only, one also cannot detect the few huge polycrystalline particles. They contribute to the X-ray intensity according to the size of their internal crystallites.

An interesting result is the formation of different crystalline phases depending on the halogen element implanted. While AgBr and AgCl are formed as crystals of the cubic NaCl structure, in the case of the co-implantation of Ag + I already in the as-implanted samples only pure silver crystallites were observed in the XRD. At a first glance this effect in Ag + I may be due to missing iodine within the SiO_2 layer for compound formation, since one deduces from TEM a significantly thinner layer, i.e., sputter effects at the surface. The sputtering of SiO_2 by iodine ions estimated from TRIM calculations is about 0.4, while the values for bromine and chlorine are below 0.3.

However, there are also some crystal–chemical aspects which may help us to understand the different tendencies towards compound formation. While AgCl and AgBr crystallize in the NaCl structure, AgI crystallizes in the zincblende ZnS structure [15]. This structural difference results mainly from geometrical reasons. The greater iodine ion occupies more space, the ionic radii ratio r_{Ag}/r_x decreases and the zincblende structure becomes energetically more favourable compared with the rock salt structure [19]. Looking into the structural details the strange coordination number of iodine with silver is only 4 (planar environment) while bromine and chlorine are sixfold coordinated with silver. Finally, the electronegativity differences between silver and bromine or chlorine are clearly higher than between silver and iodine [19]. The bonding strength will play a dominant role since the nearest-neighbour distances in AgI are between those of AgCl and AgBr. The standard enthalpies of formation for AgI (-61.8 J mol^{-1}) is about half the formation enthalpies of AgCl (-127 J mol^{-1}) and AgBr (-100.4 J mol^{-1}), respectively [20]. All these crystal–chemical aspects indicate a lower compound-forming tendency for AgI than for AgCl and AgBr. Since compound formation has already taken place during the implantation of the halogen ions, it seems that the bonding energy of AgI is not strong enough for compound formation. From the ion implantation there is an energy input to the region where compound formation can occur, which additionally hinders the process.

Another interesting feature is the observed particle size evolution in the annealing process as seen from Fig. 3. The compounds AgCl and AgBr exhibit a nearly constant mean particle size in the investigated temperature range up to 900 °C. In contrast the silver crystallites show a strong size increase when the annealing temperature is raised. Since in the samples implanted with silver only, silver crystallites are detectable by XRD only after annealing, the halogen ions as chemical species must play an important role in the crystallite formation process. It seems that this chemical influence is very effective since the particle growth during annealing of the compounds is negligible. A major amount of crystallite formation and growth took place during the implantation time. In the case of Ag + I implantation, the silver crystallites form also during implantation while, in the samples implanted only with silver, one needs an annealing process to form silver crystallites detectable by X-rays. The effect of enhancement of silver particle growth by implanting a second element has been pointed out by various workers. Also a dose dependence of colloid size was reported (see, for example, [21]). From our results it seems that there are two different effects. In the low-dose regime, one gets real nanocrystals while the colloids of 40 nm in the high-dose regime are polycrystals as observed in Fig. 4.

The sensitivity to electron irradiation in the transmission electron microscope is in contrast with the quite constant mean crystallite size of AgCl and AgBr. In both systems the effects of particle movement during the TEM investigation were observed, while similar effects do not occur in the samples with pure silver crystallites. This indicates that the crystallite growth observed is diffusion controlled. The lower diffusion rates of the larger halogen ions result in nearly temperature-independent particle size of AgX compounds while silver crystallites grow strongly.

5. Conclusions

The reported investigations show that ion implantation of silver and halogen ions Cl and Br into a SiO_2 layer results in the formation of nanocrystals of the stochiometric compounds AgX. The lattice constants of the compounds in the nanocrystallites coincide well with data tabulated for the bulk material [14]. The size of these crystallites, about 6 nm for AgBr and about 12 nm for AgCl, is not significantly altered by a subsequent annealing procedure up to 900 °C. Nanoparticles of silver halides embedded in SiO_2 are stable in size once they have formed.

In contrast the co-implantation of Ag and I into a SiO_2 layer results in silver crystallites which have formed already in the as-implanted sample. Bonding as well as crystal–chemical aspects can explain the different behaviour of the latter system. On annealing, a dramatic growth of silver crystallites from about 9 to 30 nm is observed. This annealing growth occurs also after a single implantation of silver but starts from crystallite sizes below the detection limit of XRD. This difference points out that the halogen ions play a significant role in crystallite formation and that particle growth is a diffusion-controlled process.

From cross-section TEM micrographs, one additionally learns that the particle distribution in the SiO_2 layer has a near-surface maximum in the as-implanted state. It becomes more homogeneous during annealing, but particles remain in the SiO_2 layer and do not diffuse into the Si_3N_4 layer beneath the SiO_2.

The high-resolution TEM demonstrates that most particles are of a single-crystal nature and their size corresponds well to that estimated from X-ray data. The huge particles, often described as colloids, are polycrystals and so will not exhibit the typical properties of nanocrystals.

It was demonstrated that ion implantation is a suitable tool for the production of nanocrystallites of silver and silver halides embedded in a SiO_2 layer. The possibilities of influencing the particle size and/or particle distribution within the SiO_2 layer by an annealing procedure have been shown.

Acknowledgements

We thank Mrs A. Scholz for the XRD measurements and Mrs I. Morawitz for the TEM sample preparation.

References

1. A. P. ALIVISATOS, *Science* **271** (1996) 933.
2. M. G. BAWENDI, M. L. STEIGERWALD and L. E. BRUS, *Annu. Rev. Phys. Chem.* **41** (1990) 477.
3. K. C. GRABAR, R. G. FREEMAN, M. B. HOMMER and M. J. NATAN, *Anal. Chem.* **67** (1995) 735.
4. R. F. HAGLUND Jr, L. YANG, R. H. MAGRUDER III, C. W. WHITE, R. A. ZUHR, L. YANG, R. DORSINVILLE and R. R. ALFANO, *Nucl. Instrum. Methods B* **91** (1994) 493.
5. C. FLYTZANIS, F. HACHE, M. C. KLEIN, D. RICARD and Ph. ROUSSIGNOL, *Prog. Opt.* **29** (1991) 321.
6. P. V. KAMAT, *Chem. Rev.* **93** (1993) 267.
7. R. A. WOOD, P. D. TOWNSEND, N. D. SKELLAND, D. E. HOLE, J. BARTON and C. N. AFONSO, *J. Appl. Phys.* **74** (1993) 5754.
8. K. P. JOHANSSON, A. P. MARCHETTI and G. L. McLENDON, *J. Phys. Chem.* **96** (1992) 2873.
9. A. HENGLEIN, M. GUTIERREZ, H. WELLER, A. FOJTIK and J. JIRKOVSKÝ, *Ber. Bunsenges. Phys. Chem.* **93** (1989) 593.
10. A. HAGFELDT and M. GRÄTZEL, *Chem. Rev.* **95** (1995) 49.
11. H. WELLER, *Angew. Chem.* **105** (1993) 43.
12. A. HENGLEIN, *Chem. Rev.* **89** (1989) 1861.
13. G. A. OZIN, A. KUPERMAN and A. STEIN, *Angew. Chem.* **28** (1989) 359.
14. J. F. ZIEGLER, J. P. BIERSACK and U. LITTMARK, "The stopping and Range of Ions in solids", Vol. 1 (Pergamon Press, New York, 1985).
15. Joint Committee on Powder Diffraction Standards, "Powder diffraction file (PDF-2) ", (International Center for Diffraction Data, Newton Square, PA, 1995), Set 44.
16. J. P. EBERHART, "Structural and chemical analysis of materials" (Wiley, Chichester, West Sussex, 1995) p. 203.
17. H. P. KLUG and L. E. ALEXANDER, " X-ray diffraction procedures" (Wiley, New York, 1974) pp. 656–687.
18. P. KLIMANEK, Thesis, Technische Universität Bergakademie Freiberg (1992), Chap. 4.
19. G. BURNS, "Solid state physics" (Academic Press, Orlando, FL, 1985). pp. 129–140, p. 177.
20. "CRC handbook of chemistry and physics" (CRC Press, Boca Raton, FL, 1992–1993).
21. N. MATSUNAMI, H. HOSONO, *Appl. Phys. Lett.* **63** (1993) 2050.

Received 17 July 1996
and accepted 29 July 1997